Mindanao Journal of Science and Technology Vol. 24 (Special Issue) (2026) 33-53

Performance of IMERG V07B and V06B Monthly Rainfall Data in Capturing Seasonal Magnitude and Peak Timing over Indonesia

Ravidho Ramadhan[1], Helmi Yusnaini[1], Marzuki Marzuki[1*], Robi Muharsyah[3], Mutya Vonnisa[1], Hermansah Hermansah[2], and Fredolin Tangang[4]
[1]Department of Physics
[2]Department of Soil Science and Land Resources
Universitas Andalas, Padang, 25163 Indonesia
**marzuki@sci.unand.ac.id*

[3]Center for Agroclimatology and Maritime Climate, Agency for Meteorology, Climatology, and Geophysics of Republic Indonesia, Jakarta, 10720 Indonesia

[4]Faculty of Arts and Social Sciences, Universiti Brunei Darussalam
Jalan Tungku Link, BE 1410 Brunei Darussalam

Date received: September 12, 2025
Revision accepted: August 17, 2026

Abstract

Accurate and consistent rainfall data are essential for climatological analysis and disaster risk management, particularly in regions with complex climatic dynamics such as Indonesia. This study evaluates the performance of Integrated Multi-satellite Retrievals for GPM (IMERG) Final Run version 07B (V07B) against its predecessor, version 06B (V06B), in estimating seasonal rainfall magnitude and peak timing across Indonesia over a complete 20-year period (2001–2020). Results show that IMERG V07B demonstrates significant improvements in accuracy, with lower relative bias (RB) (V06B = +19.04%; V07B = +9.68%) and root mean square error (RMSE) (V06B = 109.92 mm/month; V07B = 102.65 mm/month), along with slightly higher correlation coefficient (CC) (V06B = 0.77; V07B = 0.78). These improvements are consistent across most stations and are attributed to updates in the Goddard profiling algorithm to account more effectively for surface type and orographic influence. Despite substantial differences in monthly rainfall magnitudes between the versions, particularly over oceanic, mountainous, and coastal regions, the annual cycle phase remains relatively consistent. Harmonic fitting further enhances peak timing accuracy, increasing the proportion of correct estimates from 62.69% (V06B) to 71.64% (V07B), underscoring the suitability of V07B for seasonal rainfall analysis. Spatial assessments reveal that V07B generally produces higher rainfall estimates than V06B over land and ocean but lower values in coastal zones. Based on these findings, IMERG V07B is recommended for seasonal zoning and rainfall pattern studies in Indonesia. Further research using sub-daily and near-real-time data is needed to support high-impact applications such as flood early warning systems.

Keywords*:* IMERG V07B, Indonesia, magnitude, peak timing, seasonal

---

1. Introduction

Precipitation plays a vital role in the global energy and hydrological cycles. Accurate information on rainfall reaching Earth's surface is crucial for formulating policies that balance environmental sustainability with societal needs. In recent decades, satellite-based precipitation products (SPPs) have become a key tool for addressing the limited availability of climate observations, particularly in regions with sparse surface monitoring networks (Tang *et al*., 2018). One high-resolution SPP is derived from multi-satellite integration based on the Global Precipitation Measurement (GPM) Mission and the Tropical Rainfall Measuring Mission (TRMM), depending on the operational period (Huffman *et al*., 2015). GPM, launched in February 2014 as a joint initiative by the National Aeronautics and Space Administration (NASA) and the Japan Aerospace Exploration Agency (JAXA), has since provided continuous estimates of global precipitation (Hou *et al*., 2014).

One of the main results of GPM is the Integrated Multi-satellite Retrievals for GPM (IMERG) product, developed by NASA's Goddard Space Flight Center (Huffman *et al*., 2015). This product estimates surface precipitation from passive microwave (PMW) observations of polar-orbiting satellites processed with the Goddard Profiling Algorithm (GPROF) and then intercalibrated with the GPM Combined Ku Radar–Radiometer (CORRA) product. The merged estimates are compiled into half-hourly precipitation data at 0.1° spatial resolution and refined using a Lagrangian morphing Kalman filter interpolation scheme that incorporates infrared (IR) data from geostationary satellites. Depending on latency and morphing method, IMERG is provided in three product types: IMERG Early (approximately 4-hour latency, forward morphing), IMERG Late (approximately 14-hour latency, forward and backward morphing), and IMERG Final (approximately 4-month latency after monthly gauge data from the Global Precipitation Climatology Project (GPCP) become available).

By incorporating surface gauge corrections and post-processing, the Final product provides higher-quality estimates than the Early and Late products (Pradhan *et al*., 2022). For this reason, IMERG Final is commonly used in climatological studies, including analyses of the diurnal cycle (Tan *et al*., 2019), long-term precipitation trends and variability (Tan *et al*., 2017; Zhu *et al*., 2024b), and as input for climate and hydrological models (Jiang & Bauer-Gottwein, 2019; Meng & Zhao, 2025; Wang *et al*., 2017). Despite their lower accuracy, the faster updates of IMERG Early and Late make them highly useful for near-real-time applications, such as early warning systems for extreme rainfall events (Mazzoglio *et al.*, 2019).

In July 2023, NASA released the latest version of IMERG (version 07 or V07), which introduced several improvements to the merging algorithm, bias correction, and inter-sensor calibration, replacing the previous version (06B), released in March 2019 (Huffman *et al.*, 2023b). However, after approximately 162 problematic orbits were identified in the V07 GPROF precipitation estimates during the TRMM and GPM eras, a reprocessed version labeled IMERG V07B was issued (Huffman *et al.*, 2023b). Several studies have shown that V07B provides significant improvements in accuracy across different regions. For example, Zhu *et al.* (2024a) reported improved detection of extreme precipitation in the United States. Studies in Brazil showed reduced bias and error magnitude, along with improved critical success index scores (Rozante & Rozante, 2024; Wang *et al.*, 2023). Guo *et al.* (2024) consistently reported an increased probability of detection and a decreased average missed bias in China. Validation conducted by NASA also indicated improvements in the detection of oceanic precipitation in mid-to-high latitudes (Watters *et al.*, 2025). Nevertheless, the performance of V07B still requires extensive evaluation across various regions of the world, particularly given the dataset's recency relative to its predecessor.

Among studies comparing IMERG V07 and V06, assessments of their performance in capturing seasonal precipitation dynamics, particularly the magnitude and timing of peak annual rainfall, remain limited. This study aims to evaluate both versions' performance in representing seasonal rainfall characteristics over Indonesia, with a focus on rainfall magnitude and peak timing. Geographically and administratively, Indonesia encompasses much of the Indonesian Maritime Continent (IMC), a region characterized by diverse seasonal patterns resulting from complex interactions between monsoonal wind systems and topography (Yamanaka, 2016). However, the region's limited surface observation network continues to hinder the availability of spatially representative precipitation data (Ramadhan *et al.*, 2022d, 2022b). In this context, SPPs such as IMERG, with their relatively high spatial (0.1°) and temporal (half-hourly) resolution, offer a promising alternative to address data gaps. The study's findings are expected to inform the ongoing development of satellite-based precipitation algorithms and to support the application of IMERG in climatological research and hydrometeorological risk management across tropical maritime regions.

2. Methodology

2.1 Study Area and Rain Gauge Data

This study focuses on the IMC region, which includes the Indonesian archipelago and parts of Brunei Darussalam, Malaysia, and Singapore, as illustrated in Figure 1. Although the spatial coverage spans a large part of Southeast Asia, the primary emphasis is placed on the Indonesian islands, which comprise major landmasses such as New Guinea, Borneo, Sumatra, Sulawesi, Java, Nusa Tenggara, and Maluku. The region exhibits highly varied topography, with elevations ranging from sea level to 4,884 meters above mean sea level and consists of more than 17,000 islands. Rainfall in the IMC is characterized by strong spatial variability, with annual totals ranging from 4,000 to 7,000 mm, as reported by Ramadhan *et al.* (2022b).

Monthly rain gauge data were obtained from meteorological stations operated by the Indonesian Agency for Meteorology, Climatology, and Geophysics (BMKG). Prior to analysis, stations were filtered for data completeness during 2001–2020 and for the absence of outliers, defined as values exceeding three times the standard deviation (Ramadhan *et al.*, 2022b; 2022c; 2022d). Based on these criteria, 69 stations served as reference data to evaluate IMERG precipitation estimates. The spatial distribution of the selected stations is shown in Figure 1. This distribution is considered sufficient to capture the diversity of topographical and seasonal rainfall patterns across Indonesia.

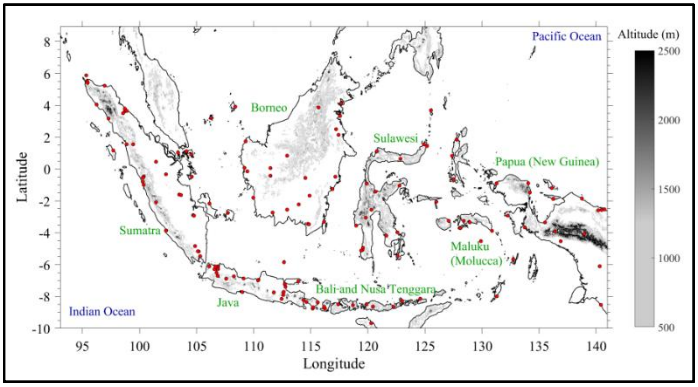

Figure 1. Topographic map of the IMC region and locations of the 69 rain gauge stations used as reference data. Elevation data were obtained from the 15-arcsecond grid provided by the General Bathymetric Chart of the Oceans (GEBCO). Blue lines indicate national administrative boundaries

Rainfall seasonality in Indonesia can be classified into three major regimes: monsoonal, semi-monsoonal, and anti-monsoonal (Aldrian & Dwi Susanto, 2003). The monsoonal pattern typically dominates southern parts of Indonesia, including southern Sumatra and Borneo, Java, Bali, Nusa Tenggara, Sulawesi, and parts of New Guinea. The semi-monsoonal pattern is observed in northern Sumatra and northwestern Borneo, while the anti-monsoonal pattern characterizes regions such as Maluku and northern Sulawesi. Accordingly, the selected rain gauge stations are considered representative for evaluating IMERG data accuracy across all major seasonal rainfall zones in Indonesia.

2.2 IMERG Final Run

In the analysis of seasonal rainfall patterns, low latency is not a critical factor, making the IMERG Final Run the most appropriate product for such applications (Pradhan *et al.*, 2022). This study compares the most recent version of IMERG Final Run (V07B) with its previous version (V06B), using ground-based rain gauge observations across Indonesia. IMERG data are freely accessible through the NASA Goddard Earth Sciences Data and Information Services Center (NASA GES DISC, 2025).

IMERG Version V07B introduces a wide range of enhancements compared to V06B. These improvements include corrections for spatial offsets, an increased cap for maximum precipitation rates, updated input algorithms, enhanced inter-sensor calibration for PMW data, and a reorganized variable-naming system (Huffman *et al.*, 2023a). Several of these updates are expected to have a substantial impact on monthly precipitation estimates. First, a significant update was made to the CORRA and GPROF V07 datasets, including fixed gridding offsets, finer surface classifications (such as coastal, oceanic, and mountainous regions), and algorithm consistency between TRMM and GPM data within CORRA. Second, the GPCP adjustment to CORRA, which was previously applied in version V06, is no longer applied over land in version V07 to address its inability to represent longitudinal variability of precipitation across land areas. Third, the estimation algorithm for IR-based rainfall was considerably improved through the implementation of the PERSIANN Dynamic Infrared–Rain Rate (PDIR-NOW) algorithm, which employs an adaptive statistical model to dynamically relate IR brightness temperature to rainfall rate.

To ensure an equitable comparison between the two IMERG versions, the data ranges were adjusted accordingly. IMERG V06B is available from 1 June

2000 to September 2021, while IMERG V07B has been extended back to 1 January 1998 based on GridSat-B1 IR data (Huffman *et al.*, 2023a). However, to maintain consistency in statistical averaging and ensure equivalent degrees of freedom, only complete calendar years were included. Thus, we compared IMERG V07B and V06B over the period from January 2001 to December 2020.

2.3 Methods

In this study, IMERG data and rain gauge observations were compared using a point-to-grid approach, selecting the nearest IMERG grid centroid for each rain gauge station for direct comparison. Three statistical metrics were employed to evaluate the accuracy of monthly IMERG estimates: the correlation coefficient (CC), root mean square error (RMSE), and relative bias (RB) (Wilks, 2011). These are common continuous statistical measures used to assess the accuracy of satellite-based estimates against ground-based measurements. The formulas for each statistical metric are presented in Equations 1, 2, and 3, as follows:

$$CC = \frac{\sum_{i=1}^{n}(y_i-\bar{y})(x_i-\bar{x})}{\sqrt{\sum_{i=1}^{n}(y_i-\bar{y})^2 \sum_{i=1}^{n}(x_i-\bar{x})^2}}, \quad (1)$$

$$RMSE = \sum_{i=1}^{n}\frac{(y_i-x_i)^2}{n}, \quad (2)$$

$$RB = \frac{1}{n}\sum_{i=1}^{n}\frac{(y_i-x_i)}{x_i}x100\%, \quad (3)$$

where n is the number of samples, x_i is the rain gauge observation, $\bar{x}$ is the mean of the rain gauge data, y_i is the satellite-based rainfall estimate, $\bar{y}$ and is the mean of the satellite estimates. A CC value of 1 indicates a perfect correlation, while the ideal values of $RMSE$ and RB are 0. Specifically, CC indicates the strength of the linear correlation between the two datasets, $RMSE$ reflects the average magnitude of the estimation error, and RB measures the degree of overestimation or underestimation in the satellite-derived rainfall compared with the observations.

To compare seasonal characteristics between IMERG V06B and V07B, the magnitude and phase (peak timing) of the annual cycle of monthly rainfall were analyzed at each grid cell. This assessment aimed to determine the capability of IMERG V07B and V06B to capture the seasonal peak and magnitude of rainfall. Two approaches were employed: the direct method (no fitting) and the harmonic-fitting method. In the direct approach, the magnitude is defined as the maximum value of the monthly rainfall climatology over one year at each grid, while the phase is defined as the calendar month when this maximum occurs. This method is explicit and sensitive to monthly fluctuations, providing an initial understanding of the differences in seasonal patterns between IMERG versions.

The harmonic-fitting approach provides smoother and more temporally consistent estimates of magnitude and phase (Ramanathan *et al.*, 2020). In this approach, the annual rainfall curve at each grid was fitted using first order (12-month) and second order (6-month) sinusoidal functions. The use of both harmonics is necessary for Indonesia's monthly rainfall patterns, which often exhibit two rainfall peaks, particularly in regions near the equator (e.g., Regions B and C), as described by Aldrian and Dwi Susanto (2003). Thus, incorporating second-order harmonic fitting allows for a more accurate representation of the annual rainfall cycle across different climatic regions.

The harmonic function as in Equation 4 was applied to the monthly rainfall as:

$$F(t) = f_0 + A_1 cos\frac{2\pi(t-T_1)}{12} + A_2 sin\frac{2\pi(t-T_2)}{6}, \quad (4)$$

where f_0 is the mean monthly rainfall, t is the selected month (1 to 12), A_1 and A_2 represent the seasonal and semi-seasonal mean-to-peak amplitudes, and T_1 and T_2 are the corresponding seasonal and semi-seasonal phases, respectively. After the fitting, the magnitude and peak timing were determined based only on the primary peak from each IMERG grid and rain gauge location. Although certain regions experience bimodal rainfall peaks, this study focused solely on the dominant peak, which contributes most significantly to annual rainfall accumulation and the risk of hydrometeorological hazards (Ramadhan *et al.*, 2022a).

All data preprocessing, statistical analyses, harmonic fitting, and figure generation were performed using MATLAB R2024b Update 1 (MathWorks, Inc., 2024). Geospatial processing of IMERG gridded precipitation, extraction of the nearest grid cell to each rain gauge station, computation of statistical performance metrics, and harmonic regression analyses were implemented using custom MATLAB scripts developed specifically for this study.

3. Results and Discussion

3.1 Evaluation of Monthly Rainfall Data

Figure 2 presents scatter plots comparing monthly rainfall values from IMERG V06B and V07B with rain gauge observations, as well as a direct comparison between V07B and V06B. The figure includes all available monthly data from 69 BMKG stations across Indonesia. The CCs between both IMERG versions and rain gauge observations are relatively similar (0.77 for V06B and 0.78 for V07B) and consistent with previous evaluations of the IMERG Final product over the IMC (Ramadhan *et al.*, 2022c). However, a notable difference is observed in RB, with IMERG V07B exhibiting a value of 9.68%, which is less than half that of IMERG V06B (19.04%). These findings are consistent with earlier studies that demonstrated the greater accuracy and improved detection capabilities of IMERG V07B at the monthly scale (Wang *et al.*, 2023; Li *et al.*, 2025).

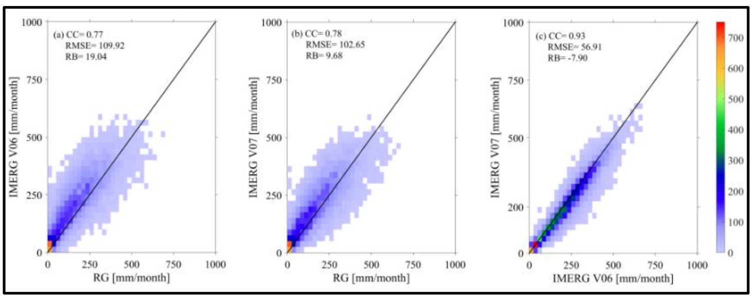

Figure 2. Scatter plots of monthly rainfall values comparing: IMERG V06B with rain gauge observations (a), IMERG V07B with rain gauge observations (b), and IMERG V07B with V06B (c)

This reduction in RB for IMERG V07B is further illustrated by a grid-to-grid comparison with V06B across grid points near BMKG stations (Figure 2c). Rainfall values from V07B are generally lower than those from V06B, reflecting a key objective of the IMERG upgrade in correcting the persistent overestimation observed in V06B (Huffman *et al.*, 2023b). This underestimation results in a substantial difference in rainfall values, with an RMSE of 56.91 mm/month. The high RMSE indicates that although the spatial patterns of rainfall may remain similar, the absolute values between the two versions can diverge considerably. This finding is consistent with those of Aksu and Yaldiz (2025), who reported that IMERG V07B has better capabilities for capturing extreme rainfall events, which V06B tends to underestimate. Additionally, the negative RB observed in many regions aligns with Wang *et al.* (2023), who found that approximately 40% of global land and ocean surfaces exhibit slightly lower rainfall estimates for V07B than for V06B. These results suggest that algorithm improvements in V07B have effectively reduced the overestimation commonly found in the previous version.

Figure 3 displays the spatial distributions of CC, RMSE, and RB for both IMERG versions at each BMKG station. The average CC across all stations is 0.81 for V07B and 0.80 for V06B, with 62.32% (V07B) and 56.52% (V06B) of stations showing CC values greater than 0.8. The mean RMSE and RB for V07B (V06B) are 96.91 mm/month (103.21 mm/month) and 15.45% (26.69%), respectively. The positive average RB values indicate that IMERG tends to overestimate rainfall at most stations, with positive-to-negative RB ratios of 2.19 (V07B) and 3.47 (V06B). The proportion of stations with absolute RB values less than 10% is 21.74% for V07B and 17.39% for V06B. These metrics collectively demonstrate that IMERG V07B generally outperforms V06B across the Indonesian region.

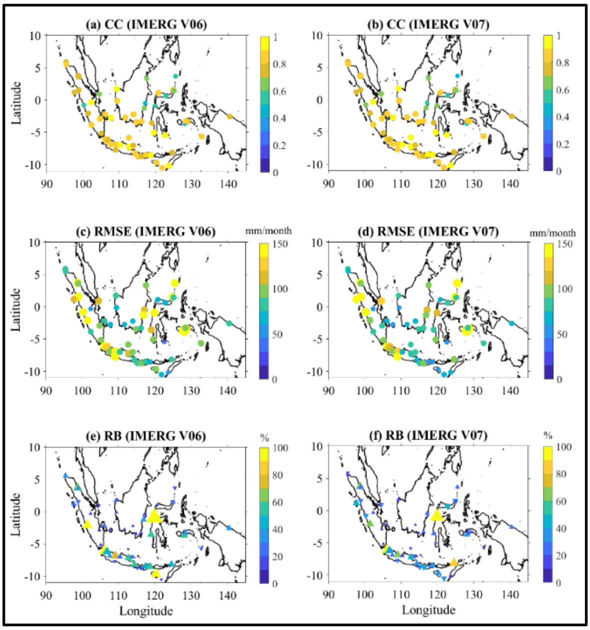

Figure 3. Spatial distributions of CC (a, b), RMSE (c, d), and RB (e, f) values derived from IMERG V06B and V07B in comparison to those from BMKG rain gauge stations across Indonesia

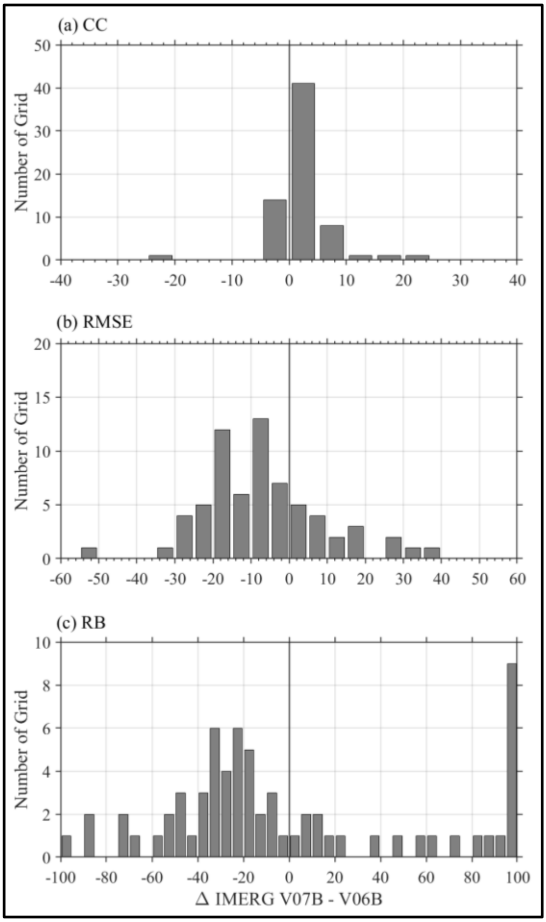

Figure 4. Histograms show the percentage differences in monthly CC (a), RMSE (b), and RB (c) values between IMERG V07B and V06B across all rain gauge stations

3.2 Evaluation of rainfall magnitude and peak timing

The determination of rainfall magnitude and peak timing in the seasonal pattern is based on the annual cycle of rainfall data. The spatial distributions of CC, RMSE, and RB values from the annual cycle at each station are shown in Figure 5. The figure demonstrates that the performance of the annual cycle derived from IMERG data is significantly better than that obtained with monthly data (Figure 3). The average values of CC, RMSE, and RB for the annual cycle from IMERG V07B (V06B) are 0.92 (0.92), 58.50 mm/month (63.83 mm/month), and 15.41% (26.68%), respectively. The very high correlation between IMERG and rain gauge data for the annual cycle indicates its strong capability to identify seasonal zones in Indonesia. Several previous studies have also used annual cycle patterns to classify monsoon zone in Indonesia (Aldrian & Dwi Susanto, 2003; Yuda *et al.*, 2021).

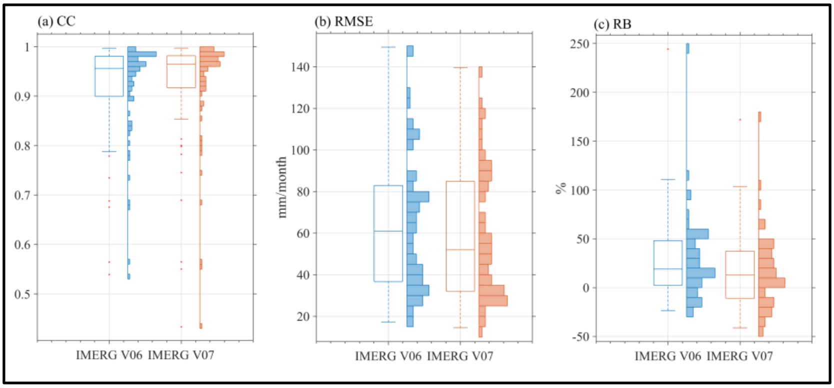

Figure 5. Boxplots and distributions of CC (a), RMSE (b), and RB (c) of the annual rainfall cycle represented by IMERG V07B and V06B compared to BMKG station observations

Figure 6 presents a comparison of magnitude and phase differences of the seasonal rainfall cycle between IMERG V07B and V06B against BMKG station observations. The analysis was conducted using two approaches: without harmonic fitting and with harmonic fitting, with the latter used to provide a smoother annual pattern. The probability distribution functions of both IMERG datasets tend to overestimate magnitude values, with peak densities of 18.58 mm/month for IMERG V07B and 43.31 mm/month for IMERG V06B. This result is consistent with the generally positive RB values shown in Figure 5. The amplitude distributions remain relatively unchanged when harmonic fitting is applied, as illustrated in Figures 6a and 6b.

The impact of harmonic fitting is more apparent in determining the phase of the rainfall peaks, as shown in Figures 6c and 6d. The percentage of grid points with accurate phase determination, defined as a difference of zero months, increased from 65.67% to 68.67% for IMERG V07B and from 62.69% to 71.64% for IMERG V06B after applying harmonic fitting. Additionally, the proportion of grids exhibiting large phase errors, defined as greater than one month, decreased from 11.94% to 7.46% for IMERG V07B and from 14.93% to 7.46% for IMERG V06B. These results indicate that harmonic fitting substantially improves the precision of rainfall peak timing interpretation from IMERG data.

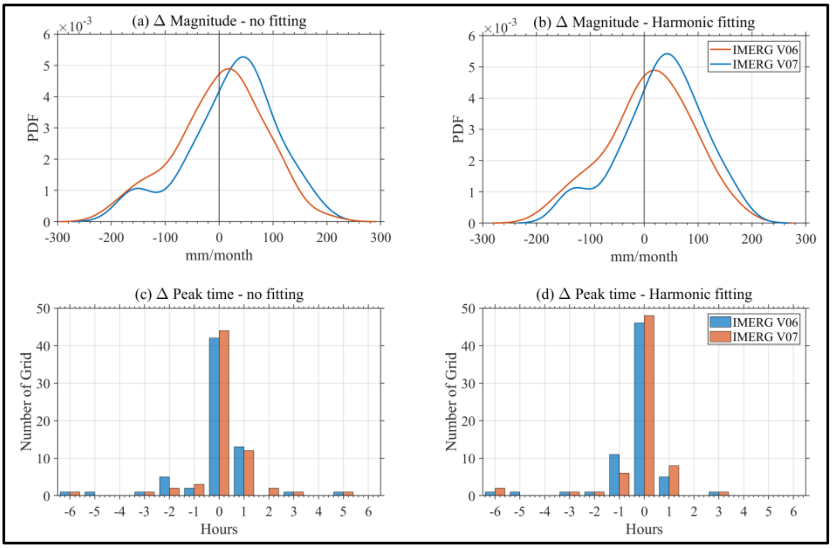

Figure 6. Differences in magnitude (a, b) and phase (c, d) of the annual rainfall cycle represented by IMERG V07B and V06B compared to BMKG station observations, based on no-fitting (a, c) and harmonic-fitting (b, d) approaches

Errors in determining the rainfall peak timing from the annual cycle may arise due to several factors. First, errors can occur at locations with a prolonged rainy season, as shown in Figures 7a and 7b, where rainfall occurs from October to February at both stations. The satellite detected the peak in November, while the rain gauge recorded it in February, resulting in a three-month difference. Nevertheless, the overall rainfall patterns were relatively similar, although IMERG tended to overestimate rainfall at station 96207 in Jambi Province. Second, errors may arise at locations with bimodal rainfall peaks, such as those observed in East Kalimantan (ID 96633) and Central Sulawesi (ID 97028) in Figures 7c and 7d, respectively. IMERG incorrectly identified the secondary peak as the main peak, leading to a large phase difference of six months compared to the rain gauge. Despite this error, the annual cycle pattern was generally well captured by IMERG. Third, peak timing errors can result when IMERG and rain gauge data do not exhibit consistent annual cycle patterns, as illustrated in Figure 7e. The discrepancy in annual cycle patterns at this station warrants further attention, even though the timing difference is only two months.

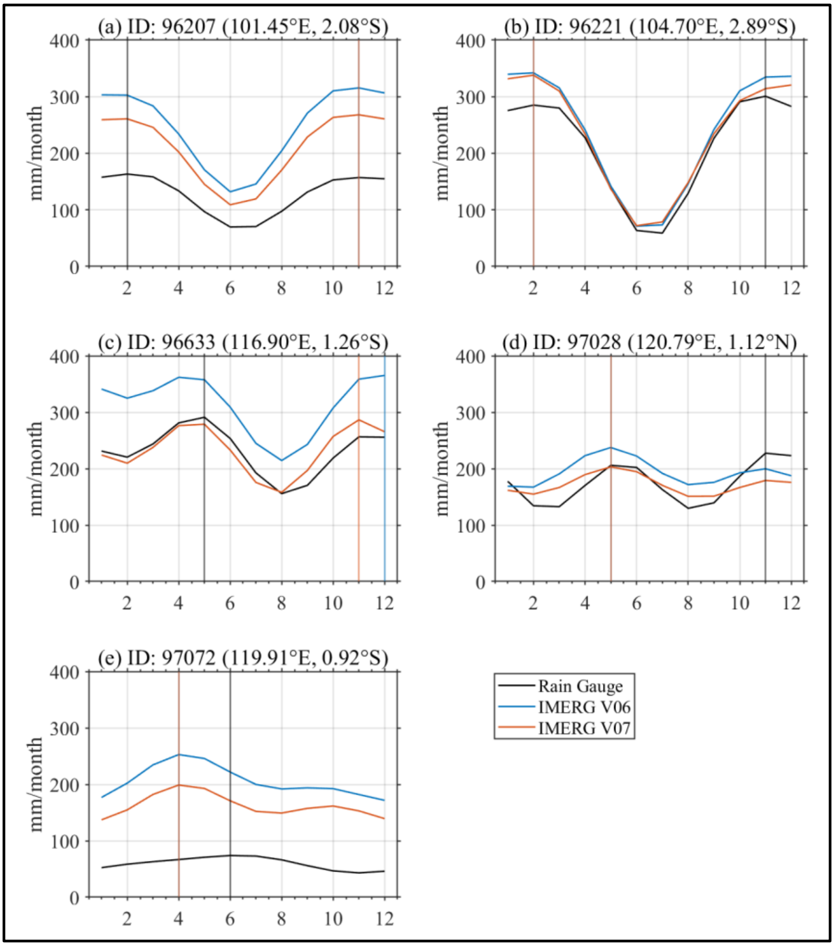

Figure 7. Annual cycle of stations with a difference of more than one month compared to the IMERG grid. The title of each panel indicates the BMKG station ID and its location

3.3 Impact of IMERG Update on Monthly Rainfall Interpretation

Sections 3.1 and 3.2 have shown that the updated IMERG V07B provides more accurate information than IMERG V06B regarding on monthly rainfall and annual cycle patterns. The differences in values between these two versions directly affect the interpretation of rainfall magnitude at each grid point across the IMC. Figures 8 and 9 present the percentage differences in monthly average rainfall values between IMERG V07B and V06B across all months. Red (blue) areas on the maps show where IMERG V07B estimates higher (lower) rainfall than V06B.

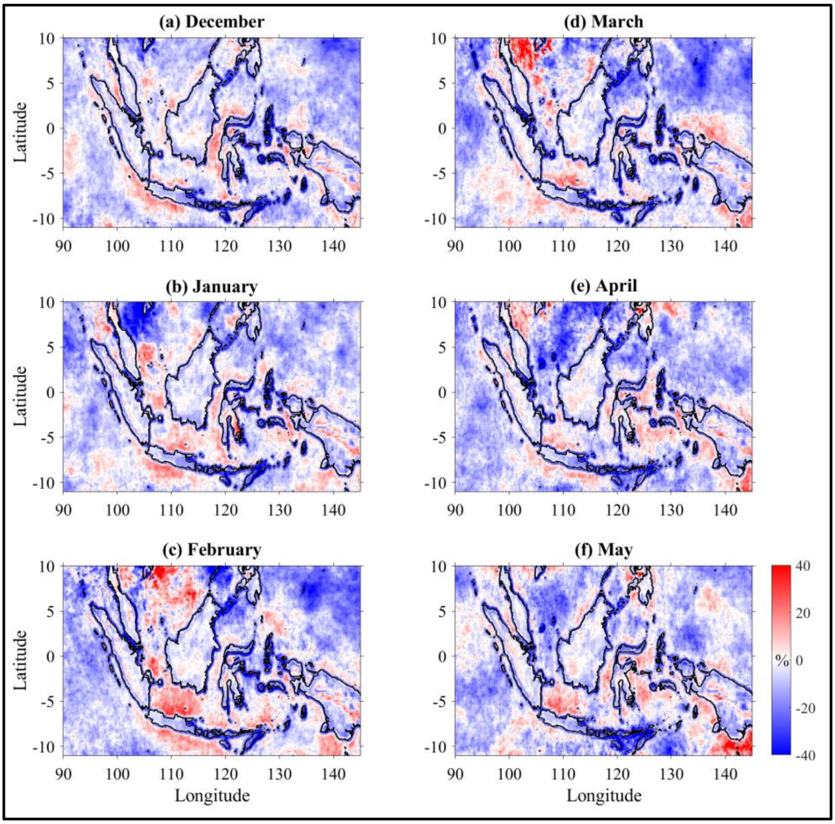

Figure 8. Percentage difference in monthly rainfall values at each grid point between IMERG V07B and IMERG V06B for December to May across the entire IMC

Notable differences between IMERG V07B and V06B are observed over ocean, land, and coastal areas (Figures 8 and 9). These differences result from the updated GPROF V07 algorithm, which classifies rainfall estimates based on surface type, with improved consideration of orographic rainfall and more detailed treatment of coastal regions. A detailed classification of the land–sea mask used in IMERG V07B can be found on the NASA website (NASA, 2025).

In general, IMERG V07B estimates higher monthly rainfall over both oceanic and terrestrial regions while providing lower estimates in coastal areas compared to V06B. The improved GPROF V07 algorithm, which accounts for orographic rainfall, is believed to have reduced missed rainfall events in mountainous areas. Enhancements in IMERG V07B over the ocean are also driven by a refined CORRA calibration process, climatological adjustments resulting from the GPCP, and correction of PMW grid geolocation errors from V06B. These improvements are particularly important over tropical oceans (Watters *et al.*, 2025), and result in substantial differences in monthly rainfall estimates between the two versions across oceanic regions in the IMC.

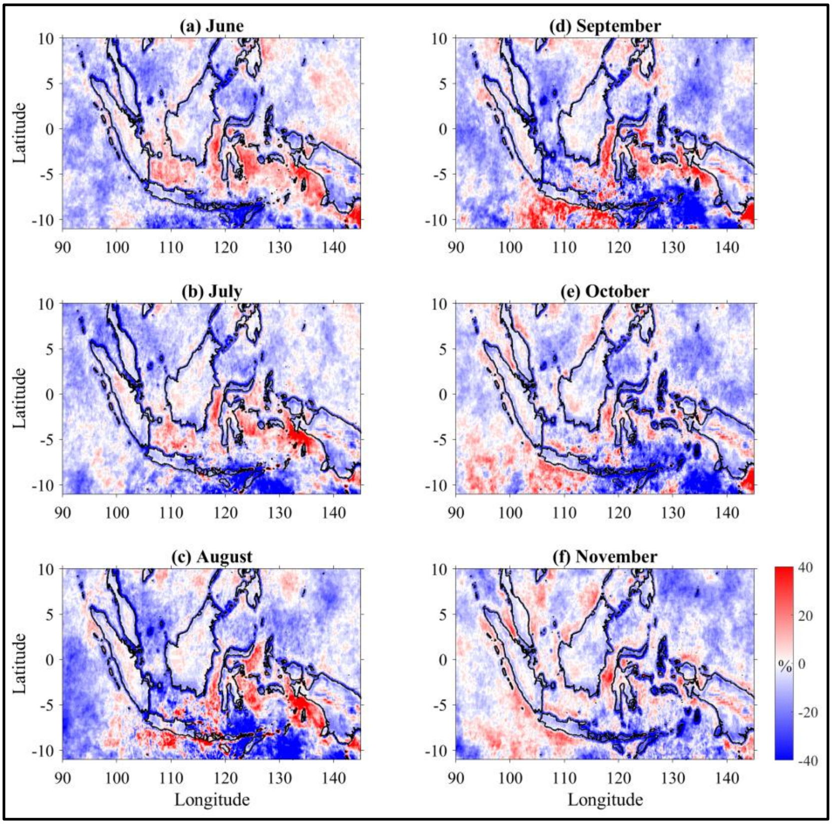

Figure 9. Percentage difference in monthly rainfall values at each grid point between IMERG V07B and IMERG V06B for June to November

The percentage differences between IMERG V07B and V06B exhibit distinct characteristics during wet and dry seasons (Figures 8 and 9). In Region C (Maluku Sea), notably higher monthly rainfall is observed during the wet season (April–September) (Aldrian & Dwi Susanto, 2003). In contrast, during low-rainfall periods, V07B estimates tend to be similar to or slightly lower than those of V06B. Conversely, in the southern maritime region of the IMC, greater positive differences occur during the boreal winter, while the differences are smaller or even negative during the dry season in June and July. These patterns suggest that the reduction of missed rainfall events and the improved hit ratio in sub-daily IMERG V07B data compared to V06B (Xiong *et al.*, 2025) significantly influence the monthly rainfall accumulation.

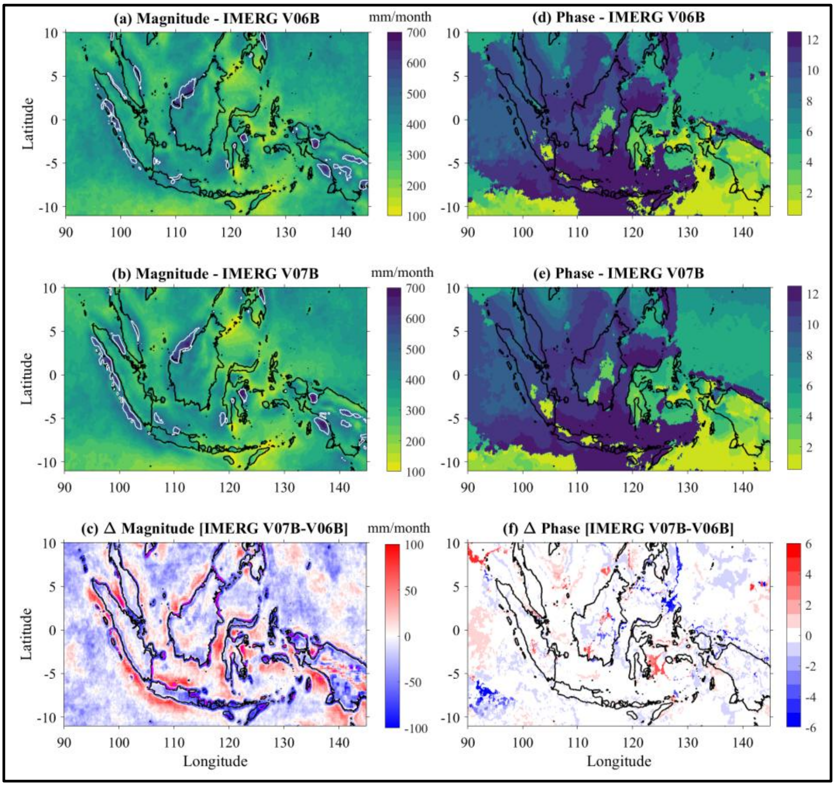

Figure 10. Magnitude (a–c) and phase (d–f) values from IMERG V06B and V07B data, along with their differences, across the entire IMC. White contour lines indicate high rainfall values above 500 mm/month, while magenta contour lines indicate large differences exceeding ±100%

The pronounced increase in monthly rainfall estimates from IMERG V07B over oceanic IMC regions during the wet season contributes to a higher magnitude in the annual cycle for those areas, as shown in Figure 10c. This difference is particularly evident over offshore regions with very high rainfall, as illustrated in Figures 10a and 10b. Additionally, in small islands such as

Bali and Nusa Tenggara, where the land–sea mask is influenced by both land and ocean, IMERG V07B tends to estimate lower magnitudes than IMERG V06B. This finding aligns with algorithm improvements in IMERG designed to reduce false detection in coastal regions (Guo *et al.*, 2024; Li *et al.*, 2025). Although there are notable differences in estimated rainfall magnitude, the differences in estimated phase between the two IMERG versions are less pronounced, as shown in Figure 10f. This observation is supported by the relatively consistent phase interpretations of the annual cycle from both datasets, illustrated in Figures 10d and 10e. Therefore, the analysis of annual cycle patterns remains reliable using either IMERG version.

4. Conclusions and Recommendation

The evaluation of monthly rainfall data reveals that IMERG V07B provides a significant improvement over V06B in estimating rainfall compared to ground-based observations across Indonesia. This enhancement is evident through lower values of RB and RMSE at most stations, along with higher CCs. Furthermore, IMERG V07B demonstrates superior performance in capturing the seasonal rainfall cycle, particularly in estimating the magnitude and timing of peak rainfall. Harmonic fitting is also shown to enhance the accuracy of peak phase detection and should be considered in future analyses. In summary, IMERG V07B is highly recommended for use in seasonal zoning and rainfall pattern analysis over the Indonesian region.

Spatial comparisons between IMERG V07B and V06B across the IMC reveal substantial differences in rainfall estimates, particularly over oceanic, mountainous, and coastal regions. IMERG V07B generally provides higher rainfall estimates over land and ocean but lower values in coastal zones. This finding is consistent with improvements introduced in the GPROF V07 algorithm, which incorporates topographic influences and refined surface classification. These notable differences in monthly rainfall magnitude directly impact the interpretation of the annual rainfall cycle. Nevertheless, the relatively small differences in the phase indicate that V07B remains reliable for seasonal-scale analyses. This suggests that although monthly rainfall values from IMERG V07B differ from those of V06B, the annual cycle patterns derived from both datasets tend to be consistent. Given the prominent updates observed in mountainous and coastal IMC regions, further investigation is warranted at sub-daily temporal scales and under extreme rainfall conditions, supported by more comprehensive ground-based observations. In addition, performance evaluations should be extended to near-real-time IMERG data to assess their potential for high-impact applications such as flood early warning systems in Indonesia.

5. Acknowledgement

This research received funding from the 2024 Fundamental Research Grants provided by the Ministry of Education, Culture, Research, and Technology of Indonesia (Kemendikbudristek, Contract no: 041/E5/PG.02.00.PL/2024). The authors would like to thank the BMKG for providing the rain gauge data for research purposes. We also thank the National Aeronautics and Space Administration for providing IMERG data.

6. References

Aksu, H., & Yaldiz S.G. (2025). Performance comparison of GPM IMERG V07 with its predecessor V06 and its application in extreme precipitation clustering over Türkiye. *Atmospheric Research*, 315, 107840. https://doi.org/10.1016/j.atmosres.2024.107840

Aldrian, E., & Dwi Susanto R. (2003). Identification of three dominant rainfall regions within Indonesia and their relationship to sea surface temperature. *International Journal of Climatology*, 23(12), 1435-1452. https://doi.org/10.1002/joc.950

Guo, H., Tian Y., Li J., Guo C., Meng X., Wang W., & De Maeyer P. (2024). Has IMERG_V07 improved the precision of precipitation retrieval in Mainland China compared to IMERG_V06?. *Remote Sensing*, 16(14), 2671. https://doi.org/10.3390/rs16142671

Hou, A.Y., Kakar, R.K., Neeck, S., Azarbarzin, A.A., Kummerow, C.D., Kojima, M., Oki, R., Nakamura, K., & Iguchi, T. (2014). The global precipitation measurement mission. *Bulletin of the American Meteorological Society*, 95(5), 701–722. https://doi.org/10.1175/BAMS-D-13-00164.1

Huffman, G.J, Bolvin D.T., Braithwaite, D., Hsu, K., Joyce, R., Kidd, C., Nelkin, E.J., Sorooshian, S., Tan, J., & Xie, P. (2023a). NASA global precipitation measurement (GPM) integrated multi-satellite retrievals for GPM (IMERG) version 07. Algorithm

Theoretical Basis Document (ATBD) Version, 47. Greenbelt, MD, United States: Goddard Space Flight Center.

Huffman, G.J., Bolvin D.T., Braithwaite, D., Hsu K., Joyce R., Xie P., & Yoo S-H. (2015). *NASA global precipitation measurement (GPM) integrated multi-satellite retrievals for GPM (IMERG).* Algorithm theoretical basis document (ATBD) version, 4(26). Greenbelt, MD, United States: Goddard Space Flight Center.

Huffman, G.J., Bolvin D.T., Joyce R., Kelley O.A., Nelkin E.J., Portier A., Stocker E.F., Tan J., Watters D.C., & West B.J. (2023b). IMERG V07 Release Notes. Greenbelt, MD, United States: Goddard Space Flight Center.

Jiang, L., & Bauer-Gottwein P. (2019). How do GPM IMERG precipitation estimates perform as hydrological model forcing? Evaluation for 300 catchments across Mainland China. *Journal of Hydrology*, 572, 486–500. https://doi.org/10.1016/j.jhydrol.2019.03.042

Li X., Liu, J., Cui W., Wang, H., Liao, A., Wang, Y., & Gao, W. (2025). Comparative evaluation of GPM IMERG V07 early, late and final run products compared to IMERG V06 in Sichuan Province, China. *Theoretical and Applied Climatology*, 156(7), 354. https://doi.org/10.1007/s00704-025-05569-x

The MathWorks, Inc. (2024). MATLAB (Version R2024b Update 1) [Computer software]. Natick, MA, USA.

Mazzoglio, P., Laio, F., Balbo, S., Boccardo, P., & Disabato, F. (2019). Improving an extreme rainfall detection system with GPM IMERG data. Remote Sensing, 11(6), 677. https://doi.org/10.3390/rs11060677

Meng, H., & Zhao, T. (2025). Evaluation of the hydrological utility of the GPM IMERG satellite precipitation products. *Atmospheric Research*, 322, 108139. https://doi.org/10.1016/j.atmosres.2025.108139

NASA GES DISC. (2025). Goddard Earth Sciences Data and Information Services Center, https://disc.gsfc.nasa.gov/datasets

NASA. (2025). IMERG land-sea mask NetCDF. Global Precipitation Measurement (GPM). Retrieved January 1, 2025, from https://gpm.nasa.gov/data/directory/imerg-land-sea-mask-netcdf

Pradhan, R.K., Markonis, Y., Godoy, M.R.V., Villalba-Pradas, A., Andreadis, K.M., Nikolopoulos, E.I., Papalexiou, S.M., Rahim, A., Tapiador, F.J., & Hanel, M. (2022). Review of GPM IMERG performance: A global perspective. *Remote Sensing of Environment*, 268, 112754. https://doi.org/10.1016/j.rse.2021.112754

Ramadhan, R., Marzuki, M., Suryanto, W., Sholihun, S., Yusnaini, H., & Muharsyah, R. (2024). Validating IMERG data for diurnal rainfall analysis across the Indonesian maritime continent using gauge observations. *Remote Sensing Applications: Society and Environment,* 34, 101186. https://doi.org/10.1016/j.rsase.2024.101186

Ramadhan, R., Marzuki, M., Suryanto, W., Sholihun, S., Yusnaini, H., Muharsyah, R., & Hanif, M. (2022a). Trends in rainfall and hydrometeorological disasters in new capital city of Indonesia from long-term satellite-based precipitation products. Remote Sensing Applications: *Society and Environment*, 28, 100827. https://doi.org/10.1016/j.rsase.2022.100827

Ramadhan, R., Marzuki, M., Yusnaini, H., Muharsyah, R., Suryanto, W., Sholihun, S., Vonnisa, M., Battaglia, A., & Hashiguchi, H. (2022b). Capability of GPM IMERG products for extreme precipitation analysis over the Indonesian Maritime Continent. *Remote Sensing*, 14(2), 412. https://doi.org/10.3390/rs14020412

Ramadhan, R., Muharsyah, R., Yusnaini, H., Vonnisa, M., Hashiguchi, H., & Suryanto, W. (2022c). Evaluation of GPM IMERG Products for Extreme Precipitation over Indonesia. *Journal of Physics*: Conference Series, 2309(1), 12008. https://doi/10.1088/1742-6596/2309/1/012008

Ramadhan, R., Yusnaini, H., Marzuki, M., Muharsyah, R., Suryanto, W., Sholihun, S., Vonnisa, M., Harmadi, H., Ningsih, A.P., & Battaglia, A. (2022d). Evaluation of GPM IMERG performance using gauge data over Indonesian maritime continent at different time scales. *Remote Sensing*, 14(5), 1172. https://doi.org/10.3390/rs14051172

Ramanathan, K., Thenmozhi, M., George, S., Anandan, S., Veeraraghavan, B., Naumova, E.N., & Jeyaseelan, L. (2020). Assessing seasonality variation with harmonic regression: accommodations for sharp peaks. *International journal of environmental research and public health*, 17(4), 1318. https://doi.org/10.3390/ijerph17041318

Rozante, J.R., & Rozante, G.I. (2024). V07B and V06B: A Comparative Study of Precipitation Estimates Across South America with a Detailed Evaluation of Brazilian Rainfall Patterns. *Remote Sensing*, 16, 4722. https://doi.org/10.3390/rs16244722

Tan, J., Huffman, G.J., Bolvin, D.T., & Nelkin, E.J. (2019). Diurnal cycle of IMERG V06 precipitation. *Geophysical Research Letters*, 46(22), 13584–13592. https://doi.org/10.1029/2019GL085395

Tan, J., Petersen, W.A., Kirstetter, P.-E. & Tian, Y. (2017). Performance of IMERG as a function of spatiotemporal scale. *Journal of Hydrometeorology*, 18(2), 307–319. https://doi.org/10.1175/JHM-D-16-0174.1

Tang, G., Behrangi, A., Long, D., Li, C., & Hong, Y. (2018). Accounting for spatiotemporal errors of gauges: A critical step to evaluate gridded precipitation products. *Journal of hydrology*, 559, 294–306. https://doi.org/10.1016/j.jhydrol.2018.02.057

Wang, Y., Li, Z., Gao, L., Zhong, Y., & Peng, X. (2023). Comparison of GPM IMERG version 06 final run products and its latest version 07 precipitation products across scales: Similarities, differences and improvements. *Remote Sensing*, 15(23), 5622. https://doi.org/10.3390/rs15235622

Wang, Z., Zhong, R., Lai C., & Chen, J. (2017). Evaluation of the GPM IMERG satellite-based precipitation products and the hydrological utility. *Atmospheric Research*, 196, 151–163. https://doi.org/10.1016/j.atmosres.2017.06.020

Watters, D.C., Huffman, G.J., Gatlin, P.N., Kirstetter, P-E., Bolvin, D.T., Joyce, R., Nelkin, E.J., Tan, J., & Wolff, D.B. (2025). A Diagnosis of Oceanic Precipitation in IMERG-GMI. *Journal of Hydrometeorology*, 26(4), 459–480. https://doi.org/10.1175/JHM-D-24-0137.1

Wilks, D.S. (2011). Statistical methods in the atmospheric sciences. California, United States: Academic press.

Xiong, J., Tang, G., & Yang, Y. (2025). Continental evaluation of GPM IMERG V07B precipitation on a sub-daily scale. *Remote Sensing of Environment*, 321, 114690. https://doi.org/10.1016/j.rse.2025.114690

Yamanaka, M.D. (2016). Physical climatology of Indonesian maritime continent: An outline to comprehend observational studies. *Atmospheric Research*, 178, 231-259. https://doi.org/10.1016/j.atmosres.2016.03.017

Yuda, I.W.A., Osawa, T., Nagai, M., & Prasetia, R. (2021). The Regionalization of Indonesian Maritime Continent Rainfall based on Integrated Multi-satellite Retrievals for GPM (IMERG). IOP Conference Series: Earth and Environmental Science, 893(1), 12065. https://doi.org/10.1088/1755-1315/893/1/012065

Zhu, S., Li, Z., Chen, M., Wen, Y., Gao, S., Zhang, J., Wang, J., Nan, Y., Ferraro, S.C., & Tsoodle, T.E. (2024a). How has the latest IMERG V07 improved the precipitation estimates and hydrologic utility over CONUS against IMERG V06?. *Journal of Hydrology*, 645, 132257. https://doi.org/10.1016/j.jhydrol.2024.132257

Zhu, S., Li, Z., Chen, M., Wen, Y., Liu, Z., Huffman, G.J, Tsoodle, T.E., Ferraro, S.C., Wang, Y., & Hong, Y. (2024b). Evaluation of IMERG climate trends over land in the TRMM and GPM eras. *Environmental Research Letters*, 20(1), 014064. https://doi.org/10.1088/1748-9326/ad984e